Faraday Discussions

Accepted Manuscript

This manuscript will be presented and discussed at a forthcoming Faraday Discussion meeting. All delegates can contribute to the discussion which will be included in the final volume.

Register now to attend! Full details of all upcoming meetings: http://rsc.li/fd-upcoming-meetings

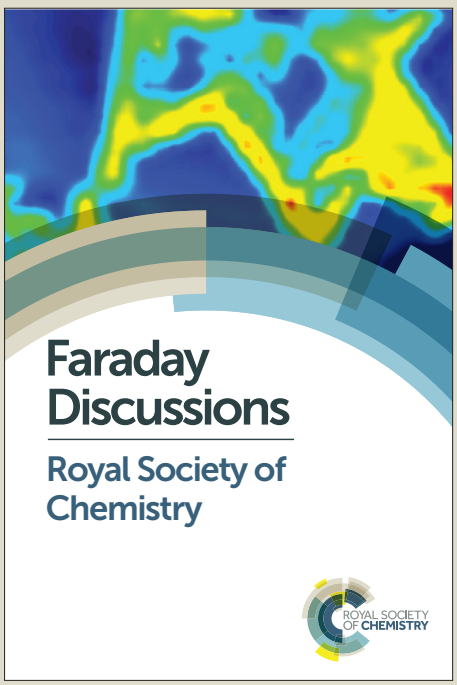

This is an *Accepted Manuscript*, which has been through the Royal Society of Chemistry peer review process and has been accepted for publication.

Accepted Manuscripts are published online shortly after acceptance, before technical editing, formatting and proof reading. Using this free service, authors can make their results available to the community, in citable form, before we publish the edited article. We will replace this *Accepted Manuscript* with the edited and formatted *Advance Article* as soon as it is available.

You can find more information about *Accepted Manuscripts* in the Information for Authors.

Please note that technical editing may introduce minor changes to the text and/or graphics, which may alter content. The journal's standard Terms & Conditions and the Ethical guidelines still apply. In no event shall the Royal Society of Chemistry be held responsible for any errors or omissions in this *Accepted Manuscript* or any consequences arising from the use of any information it contains.

ROYAL SOCIETY OF CHEMISTRY

www.rsc.org/faraday_d

Single Molecule Fluorescence Resonance Energy Transfer Scanning Near-field Optical Microscopy: potentials and challenges

S. K. Sekatskii[a], K. Dukenbayev[ab], M. Mensi[ac], A. G. Mikhaylov[a], E. Rostova[a], A. Smirnov[a], N. Suriyamurthy[ad], and G. Dietler[a]

[a]*Laboratoire de Physique de la Matière Vivante, EPFL, CH1015 Lausanne, Switzerland*
[b]*Present address: "National Laboratory Astana" PI, "Nazarbayev University" AEO, Kabanbay batyr avenue, 53, Astana, 010000 Kazakhstan*
[c]*Present address: Optics and Photonics, KTH Isafjordsgatan 22, 16440 Stockholm, Sweden.*
[d]*Permanent address: Radiological Safety Division, Indira Gandhi Centre for Atomic Research, Kalpakkam, India.*

A few years ago single molecule Fluorescence Resonance Energy Transfer Scanning Near-Field Optical Microscope (FRET SNOM) images were demonstrated using CdSe semiconductor nanocrystal – dye molecule as donor-acceptor pair. Corresponding experiments reveal the necessity to exploit much more photostable fluorescent centers for such imaging technique could become a practically used tool. Here we report the results of our experiments attempted to use for FRET SNOM nitrogen vacancy (NV) color centers in nanodiamond (ND) crystals which are claimed to be extremely photostable. All attempts were unsuccessful, and as a plausible explanation we propose the absence (instability) of NV centers lying close enough to the ND border. We also report improvements in SNOM construction that are necessary for single molecule FRET SNOM imaging. In particular, we present the first topographical images of single strand DNA molecules obtained with fiber-based SNOM. Prospects of the use of rare earth ions in crystals, which are known to be extremely photostable, for single molecule FRET SNOM at room temperature and quantum informatics at liquid helium temperatures, where FRET is a coherent process, are also discussed.

1. Introduction

Fluorescence Resonance Energy Transfer Scanning Near-field Optical Microscopy (FRET SNOM), which idea is illustrated in Fig. 1, consists in a division of a donor – acceptor FRET pair between a SNOM tip and a sample[1,2]. If donor fluorescent centers of the imaging tip are excited and the fluorescence of the acceptor centers of the sample is monitored (or vice versa) when the tip is scanning along the sample surface, the spatial resolution is governed not by the aperture size of the microscope but by the value of a characteristic FRET (Förster) radius R_0. The latter for typical donor – acceptor pairs ranges 3 – 7 nm[3-5] and thus the spatial resolution of SNOM can be ten times improved without the loss of sensitivity: the resolution of a "standard" aperture SNOM is governed by an aperture size which can not be made essentially smaller than 50 nm due to the very rapid decrease of the light transmission through the tip when aperture is decreasing[6-8].

To achieve the subtip spatial resolution with this method, we do not need to work with its single molecule version: only a (partly filled) cylinder with the radius $r = \sqrt{2RR_0}$ contributes to the signal[2], see Fig. 1, left. Here R is a radius of the curvature of a SNOM probe apex which is typically equal to 50-100 nm, and usually exactly this radius determines the spatial resolution. It is easy to see that $r << R$.

Immediately after an idea of the method has been proposed[1], the corresponding experiments started and nanolocal FRET SNOM measurements and FRET SNOM images have been reported by a number of research groups using such fluorescent centers as dye molecules[9-12], semiconductor nanocrystals[13-15] and *F*-aggregated color centers in LiF crystals[16]. Finally, in 2008 these efforts lead to observation of single molecule FRET SNOM images in an experiment where 4.8-4.9 nm CdSe nanocrystals (this is a core diameter; the core was covered with a protective 1-2 nm thick ZnS layer) deposited onto a glass slide surface were used as donors and Alexa Fluor 594 dye molecules (Molecular Probes, Oregon, USA) contained inside thin PMMA coating over SNOM tip apex were used as acceptors[17].

However, the results reported in Ref.[17] remain isolated and did not lead to the real appearance of single molecule FRET SNOM imaging method. We still prefer to characterize the current situation as "*towards single molecule FRET SNOM*", and the reason for this is the limiting photostability of dye molecules and semiconductor nanocrystals used for imaging. (Our FRET SNOM researches involving CdSe nanocrystals do *not* confirm that their photostability is much larger than that of rhodamine dyes contrary to what is often stated). For typical optical absorption cross section of a single fluorescent centre $\sigma \cong 10^{-16}\ cm^2$, photon energy $h\nu \cong 3 \cdot 10^{-19}\ J$ and near-field illumination intensity $I \cong 10^3\ W/cm^2$, the photostability (a good one) of $N_{phst} \cong 10^7$ cycles determines the time of life of a center equal to $t = \frac{N_{phst} h\nu}{I\sigma} \cong 30\ s$. In practice, this means that a special construction of microscope enabling quite fast scanning should be exploited, and extreme precautions to avoid

the premature killing of acting single FRET centre by light (such as opening of light source only after the scanning already started, etc.) should be taken to observe single molecule FRET SNOM images; and despite all this, such an observation still requires certain luck.

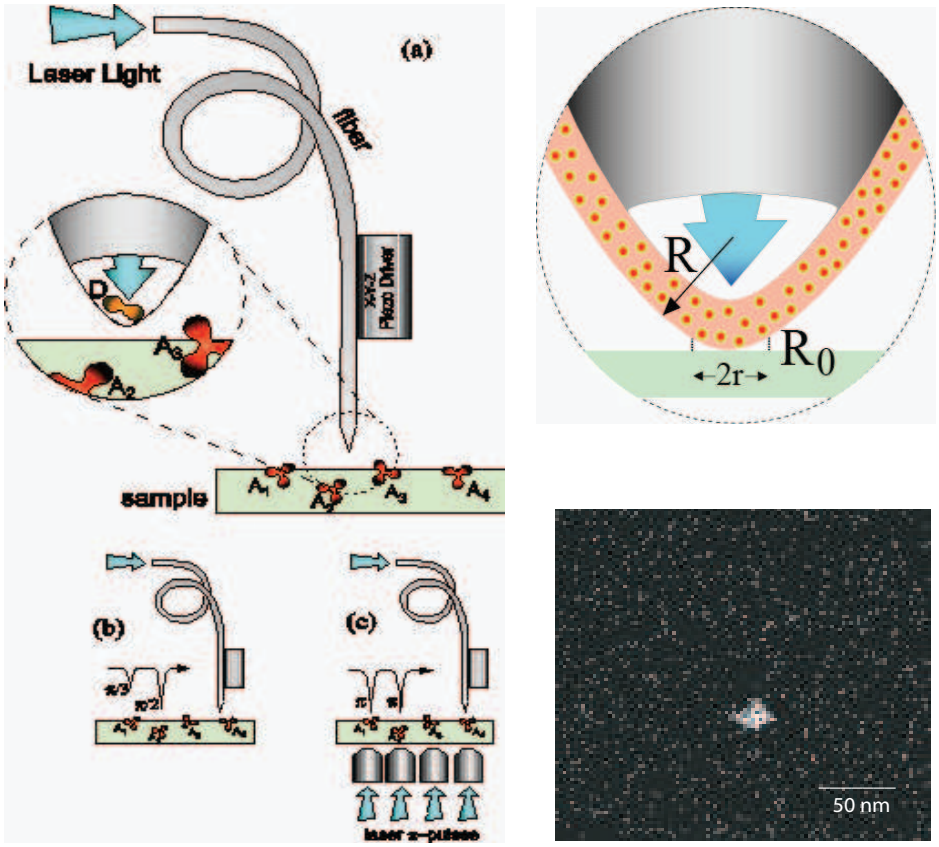

Fig. 1. Left (reproduced from Ref.[22], with permission) (a) Illustrating an idea of FRET SNOM approach, single fluorescent centre case. Preparation of non-local entangled Greenberger-Horn-Zeilinger three-particle state (b; distances between donor and acceptor centres are changed in a controllable fashion to ensure desirable *partial* excitation transfer from donor to acceptor, we name this $\pi/3$ and $\pi/2$-pulses) and CCCNOT operator (c; donor is initially excited and remains excited if and only if the acceptors were initially excited by resonant light π-pulses) for the case of coherent FRET is shown. Right: Illustrating the spatial resolution of FRET SNOM working at many molecules level (up); single molecule FRET SNOM image obtained for CdSe nanocrystal – dye molecule donor acceptor pair (below, reproduced from Ref.[17], with permission).

The situation would change dramatically provided much (say, two orders of magnitude) more photostable fluorescent centres are used. Naturally, this suggests to attempt famous nitrogen vacancy (NV) defect centres in nanodiamond (ND) crystals, claimed to be extremely photostable[18-21], in FRET SNOM imaging, and such researches do started not only in our group but also elsewhere. Still, to the best of our knowledge, this activity did not result in obtaining of single molecule FRET SNOM images. The apparent reasons for this and possible further steps are discussed in our paper together with necessary improvements of scanning near-field microscope made specially to achieve this aim. In particular, we present what we believe is the first and still unique observation of topographical images of *single strand* DNA molecules with an optical fibre-based SNOM device.

Other extremely photostable fluorescent centres are rare-earth ions in crystals, and they naturally should be considered as perspective for FRET SNOM as well. Exploitation of rare earth ions in crystals looks interesting also from the viewpoint of quantum computing applications of FRET SNOM[22]. In the case of liquid helium temperatures, for numerous optical transitions of rare-earth ions in crystals decoherence (dephasing) time becomes quite comparable with the radiative decay time[23-26]. In some cases it can attain the value of a few milliseconds while microsecond decoherence times are a widespread phenomenon. At such conditions, FRET is a coherent process and the quantum dynamics of the system is well approximated by a standard dynamics of a two-level quantum system: the excitation energy flows back and forth between donor and acceptor, and for typical cases the period of this energy exchange is equal to the radiative decay time when the donor – acceptor distance is around 20 nm. Hence all the parameters required (a few nanometers precision of the tip – sample motion at the time scale of a few microseconds, liquid helium temperatures) are quite feasible with modern Scanning Probe Microscopy (SPM) technique[22], and different protocols how to perform basic quantum computing operations (some of them are illustrated in Fig. 1) can be proposed.

The prospects of use of rare-earth ions in crystals for both incoherent and coherent FRET SNOM will be briefly discussed in the last section of the paper.

2. SNOM device: fast scanning and ultralow acting forces

The Scanning Near Field Optical Microscope used in our researches has been discussed earlier[27] so here we only rather briefly characterize its peculiarities important for single molecule FRET SNOM imaging. This microscope is capable of fast scanning necessary to (partly) overcome the severe photostability problem. The main tool to achieve this is the use of an original "double resonance principle": working frequency of the tuning fork (which is close to 32 756 Hz) coincides with the second resonant frequency of lateral dithering of a free-standing part of the fiber beam[28]. The use of proprietary low noise, precise and fast electronics measuring the resonance frequency f_{res} and Q-factor of a tuning fork[27], earlier designed to be

exploited essentially with the sensors "tuning fork and AFM cantilever glued upon it"[29] is also important. The double resonant montage, which requires careful control of the length of the free standing part of the fiber beam and of the position of a thin (40 micron-thick) glass rod connecting the fiber probe with one of the tuning fork's prongs, as well as careful assembling (gluing) of all parts, enables to routinely achieve the quality factor of the sensor ranging 3500 – 5500, and its exploitation results in the force sensitivity as small as 30 pN in a bandwidth of 300 Hz. This large force sensitivity enabled to image double strand DNA molecules using both glass and plastic[30] fiber-made SNOM probes.

Even better performance of the microscope was achieved using electronics of Nanonis GmbH, Zürich, Switzerland, specially jointly adapted by our Laboratory and the Company to work with SNOM exploiting high *Q*-factor probes. Probes were oscillated at (or close to) the resonance frequency with a 1-5 mV_{rms} sinusoidal voltage applied to the tuning fork's electrodes which caused a current of the order of 20 nA_{rms}. The current is amplified by a current-voltage preamplifier (Nanonis TFPA-3) with a gain of 1 V/μA corresponding to a trans-impedance of 1 MΩ. The bandpass ranges from DC to 150 kHz, and the noise level in the 10 Hz to 1 MHz window was smaller than 0.27 mV. Different glass fiber-made SNOM probes, including those commercially available from KDP company, Moscow, Russia, aperture probes modified in Scanning Electron Microscope vacuum chamber to grow ultrasharp whiskers onto their apex[31], or home-etched in HF solution following the tube-etching approach[32,33] probes, were used.

In Fig. 2 we present what we believe are the first and unique topographical images of *single strand* DNA molecules obtained using fiber-based SNOM technique. DNA sample preparation was the same as discussed earlier[34]. Very briefly, double strand linear DNA sample (Fermentas, Lambda Mix Marker 19) was diluted to the concentration of 1 μg/ml in a 1 mM TRIS buffer solution at pH=7.8. The single-strand DNA was prepared by heating up the linear DNA solution at 60°C for 1 minute, after what the 10 μl aliquot of the DNA solution was deposited onto mica modified by 3-aminopropyltriethoxysilane (APTES; AP-mica), incubated for 60 seconds, rinsed with 500 μl of nanopure water and gently dried. AP-mica was prepared by treating a freshly cleaved mica surface with a solution of 0.05% APTES in water for 1 minute, rinsed thoroughly with nanopure UHQ water (USF Elga, High Wycombe, England) and dried with dry air.

Another important for the applications at question characteristic of the Microscope is its capability of time-gated detection of the optical signal using either an external TTL pulse triggering a light source (laser) and then, with an appropriate delay regulated by SNOM electronics, also the photon detector. Alternatively, SNOM electronics itself generates a TTL pulse to trigger an external laser source and (again, with an appropriate delay) photon detector. In both cases, delay times can be regulated in a broad range with a quantum of 25 ns. This option was proved to be useful for imaging fluorescent nanospheres using 10 – 100 μs-

duration light pulses obtained exploiting an acousto-optical modulator with cw Nd:YAG laser at 532 nm[27], and afterwards also with a nanosecond (<2 ns duration) pulsed Nd:YAG laser at 532 nm.

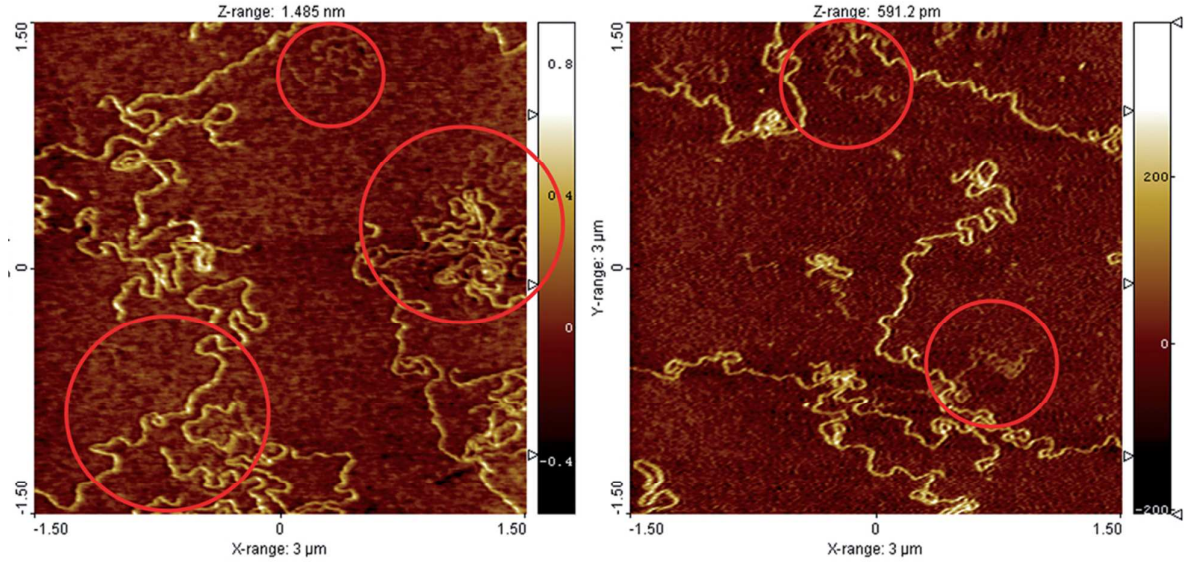

Fig. 2. Topographical images of DNA molecules deposited onto APTES-modified mica surface (see text for details) obtained with SNOM. Single strand parts of DNA are highlighted with red circles.

The following consideration is at place here. This is known and broadly accepted in the area of near field optics (and fully corresponds to our own experience) that, when working with cw laser, light intensity at the subwavelength-size aperture of SNOM probe cannot exceed the value around $I \cong 10^3\ W/cm^2$, and this corresponds to the laser power of ca. 0.5 – 3 mW at the entrance of the probe made of single-mode glass fiber. For larger values, the probe can be easily damaged and burned by light. Correspondingly, when measuring the signal caused by single fluorescent center, we can have around

$$n = \eta \frac{I\sigma}{h\nu} \cong 3 \cdot 10^3 - 10^4 \qquad (1)$$

photocounts per second. Here η is an overall efficiency coefficient which includes all factors such as fluorescence quantum yield, photon collection- and detector efficiencies; above it is taken ranging 0.01-0.03 (a good value indeed) while all other parameters are the same as were used in Introduction. This value is one-two orders of magnitude larger than a typical dark noise level of single photon detector, but experimentally it is quite difficult to diminish the parasitic noise signal, caused essentially by unavoidable stray light, already to this value, not to mention to sufficiently lower one.

Let us see what changes if pulsed laser excitation is used instead of a continuous one. For such case, one still should use the same average value of the

total laser energy passing through the fibre during 1 second, and consequently the same average value of intensity I, to avoid fibre damage: this damage is essentially a thermal effect (we have checked up this circumstance with microsecond[27] and afterwards also nanosecond laser pulses; the damage threshold do depends only on the total power introduced into the SNOM probe). However, now the gated detection drastically decreases both dark detector- and (a part of) stray light-related noise levels. Earlier[27] we have considered the situation when the laser pulse duration t_p is much larger than the single fluorescent center radiative decay time t_{fl}. Then for the laser pulse repetition rate F and gate duration T this decrease is equal to $(FT)^{-1}$ while the overall signal level is unchanged, and this has been demonstrated experimentally. If, however, as it takes place now, $t_p < t_{fl}$, the total effect is smaller because the decrease of noise level is partly "compensated" by the decrease of the signal. The number of optical absorption events per second is $N = 1/\tau = \frac{I\sigma}{h\nu}$, and it is clear that using pulsed laser with the same average intensity I and pulse repetition rate F, if $F<N$, one saturates an optical absorption of the fluorescence center during a single pulse. However, for single emitting centre the signal level now is just ηF hence the increase of signal to noise ratio is given by τ / t_p. For T=25 ns and other parameters given above we still have an improvement of two orders of magnitude.

Of course, this gating cannot diminish the noise coming from "not fully suppressed laser light itself" and caused by it very fast parasitic fluorescence "of everything", but note that now we need not any more so strong light intensity: this is useless to oversaturate the transition during single pulse, it just needs to be saturated. This decrease of laser power leads to the corresponding decrease of the noise directly caused by excitation light. Certainly, a decrease of the signal level paid for the improvement of signal to noise ratio necessitates slower scanning during the imaging.

3. Single Molecule FRET SNOM: room temperature case

3.1. From CdSe nanocrystals to colour centres in nanodiamond crystals

In Introductory Section we have already briefly discussed the first single molecule FRET SNOM images, their limitations and motivation to use ultraphotostable NV color centers in nanodiamond crystals. Indeed, these same color centers were considered as prospective from the very beginning of FRET SNOM research[1], while their first use in SNOM area (as local fluorescence source) goes back to 2000[35]. The same motivation promotes the use (or attempts to use) of diamond NV fluorescent centers in many other areas. As an example, let us only underline their rather successful application in Stimulation Emission Depletion Microscopy field[36,37] where exactly this same photostability problem defines the ultimate spatial resolution achievable.

Photophysics of NV color centers is still not fully understood and remains

debated. Especially, this is valid when details concerning the charge states NV^0 and NV^- of nitrogen vacancy and their inter-transformations (either spontaneous or specially induced) are considered. Nowadays, this is almost exclusively NV^- state which is exploited, but it is worthwhile to note that NV^0 state also was discussed as a very prospective candidate for quantum informatics – related applications[38]. However, FRET SNOM imaging at room temperature does not involve any coherent and spin properties of the emitting center, hence from the very beginning we decided not to target certain particular charge state but to search for imaging caused by either NV^0 (luminescence band essentially in 570-700 nm spectral range) or NV^- (620 – 750 nm) states. Indeed, detailed time-resolved experiments with single NV centers show the photo-switching from neutral to negatively charged state of NV as well as reverse photochromic transformation with the time constant ranging 0.3 – 3.6 microseconds (2.1 μs in average) under dark conditions[39]; earlier, photochromism has been shown for bulk samples[40]. There are no two different types of defects but "both fluorescence bands originate from the same defect" and "continuous switching between two charge states exists"[39]. The laser ionization of nitrogen donors present in the vicinity of the NV defect is a plausible mechanism of NV^0 to NV^- conversion, and this means that such a process should be strongly dependent on the concrete properties of colored ND and laser illumination conditions. In a sense, NV^0 state should be considered as a "main" one which is initially present (and consequently, its luminescence should be "always" observed) while NV^- state should first be created by the irradiation itself so that its observation may be not guaranteed at all.

Following this paradigm, different laser dye molecules (oxazine 1, oxazine 750, Rhodamine 800)[41] were systematically tried in our experiments as potential acceptors for either NV^0 or NV^- donors. This circumstance makes mostly irrelevant still much debated question to what extent the neutral charge state is preferable at small (a few nanometers) distances from the ND particle surface and to what extent (if any) the NV^-/NV^0 concentration ratio can be influenced by surface modification or other means[42-46].

Two different sources of bright colored nanodiamond crystals were used in our experiments. The first were solutions (for simplicity, here and below we use the word "solution" to describe ND particles water-based suspensions) and powders of nanodiamond crystals purchased from Microdiamant AG, Lengwill, Switzerland, with the average size of 25 nm or 50 nm and the communicated concentration of the nitrogen vacancies around 25 - 100 p. p. m.

To color them, the powder of these diamonds (25 nm-size) has been introduced into specially prepared "flat" envelopes made from thin 50 micron-thick *Al* foil and irradiated by 2.4 MeV-energy electron beam in the accelerator ILU-6 (average current 2 – 3 mA) of the Institute of Nuclear Physics Siberian Branch of Russian Academy of Sciences, Novosibirsk, Russia. The total dose of the irradiation was set to be equal to $1 \cdot 10^{18}\ e^- / cm^2$ (for one half of the sample) and $2 \cdot 10^{18}\ e^- / cm^2$ (another

half). Afterwards, the irradiated diamond dust has been thermally annealed in technical vacuum (around 1 mTor) at the temperature of 750 – 800 ^{0}C during two hours. No further treatment aiming to remove graphite layers possibly covering the as-irradiated nanodiamonds[37,47] was undertaken. This procedure is more or less similar to those suggested in many other papers starting from the classic Davis and Hamer paper[48]. It was reported that for $3 \cdot 10^{17}\ e^- / cm^2$ and 1.5 MeV dose and energy of electron beam, roughly 1 NV center in a 30 nm - diameter sphere has been created[49,50] thus we anticipated somewhat similar results for our case.

Second sample of fluorescent nanodiamonds were commercially available coloured nanodiamonds in solution obtained from L. M. Van Moppes & Sons SA, Geneva, Switzerland, (average size of 65 nm, concentration of NV colour centres was not communicated), and Adamas Nanotechnologies, Inc., Raleigh, NC, USA, Companies. For the latter, the content of in average 1 - 4 NV fluorescent centres in one 40 nm-size nanodiamond particle has been indicated.

In Fig. 3 we present fluorescent spectra of water solution of 40 nm-diameter nanodiamonds obtained for different excitation wavelengths (results for other solutions of fluorescent ND were similar with appropriate scaling). The first conclusion from these data is the very strong presence of all possible types of light "scattering" in the recorded signal. (We use this word as a generic term to describe any type of observed signal which is *not* NV fluorescence band(s); we did not perform detailed studies to trace out its origin deeming this irrelevant for our purposes to construct FRET SNOM. Unfortunately, existence and importance of this type of optical signal are almost never reported in the literature). The second conclusion is the strong dependence of the efficiency of the excitation of NV fluorescence band, lying in the region of 580 – 700 nm, on the excitation wavelength.

Direct comparison of the fluorescent signal obtained from a solution of colored 40 nm-diameter ND with that of Sulphorhodamine B water solution[41] excited in the spectral range 530 – 570 nm, accepting for both the same quantum yield and optical absorption cross-section of $3 \cdot 10^{-17}\ cm^2$ at maximum for NV centers[51] (the latter is equal to $6 \cdot 10^{-17}\ cm^2$ for dye molecules at the wavelength of 532 nm[41]), leads to the estimation of the average number of NV centers in one ND particle as 0.4-0.8 thus being indeed not too far from the data communicated by the producer. Similar estimations give for 25 nm-diameter ND colored in Novosibirsk the value around 0.2 – 0.4.

From the recorded graphs, the very appearance of NV fluorescence band (apparently, this is NV^0 band) was unambiguously attested only in the spectral range of excitation from roughly 540 to roughly 610 nm; for shorter wavelengths the excitation is much less effective, and it is strongly obscured by "light scattering signal". Still NV luminescence is definitely excited by nanosecond pulsed 532 nm laser, as was attested by observation of fluorescence kinetics with the time of life equal to ca. 12 ns thus quite comparable with the literature data[18-21] (Time Correlated Single Photon Counting module PicoHarp 300, PicoQuant, Berlin,

Germany, was used); similar kinetics have been observed for ND samples in solution, in thin polymer films and in thin layers of polymer deposited onto an aperture SNOM tip apex; see below. The efficiency of excitation of NV-centers fluorescence by pulsed ns 532 nm laser (as well as by cw 514 nm laser) is difficult to estimate. Our data suggest for the corresponding cross section the value something like one order of magnitude smaller than at maximum, i.e. around $3 \cdot 10^{-18}\ cm^2$. (Note the value $1 \cdot 10^{-17}\ cm^2$ reported for optical excitation cross section at this wavelength in Ref.[48]).

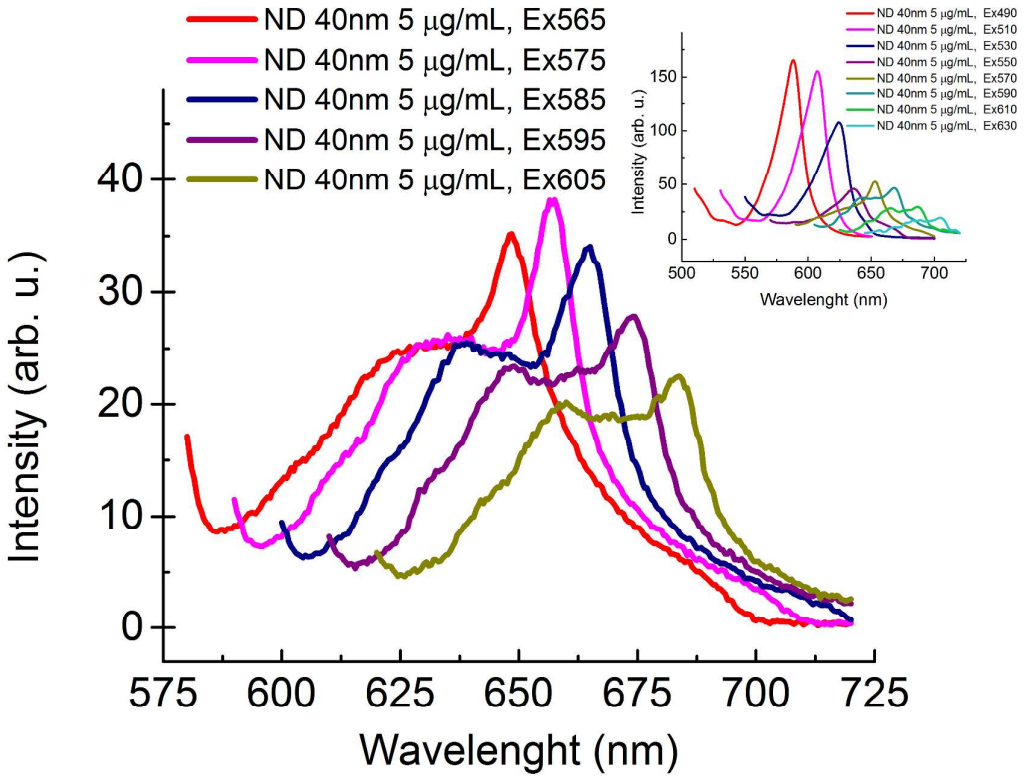

Fig. 3. Optical signal recorded at different excitation wavelengths for 5 μg/ml water-based suspensions of colored 40 nm-size nanodiamond particles. Known NV^0 luminescence band (590 – 700 nm) is seen when excited in the spectral range 540 – 630 nm and not seen when excited at shorter wavelengths, see the insert. Spectra are recorded by Jasco FP-8500 spectrofluorimeter (Easton, MD, USA) with a detector sensitive in 200 – 750 nm spectral range which may obscure observation of the red part of NV centers fluorescence.

For FRET SNOM experiments, the distance between donor and acceptor should be smaller than the Förster radius R_0. This adds one more constrain which from the first glance does not look too restrictive: for a spherical particle of radius R, only those color centers which lie at the distances larger than R-r with $r<R_0$ from the center, can contribute. For R=12.5 nm and r=3 nm this signifies that more than one half of all NV centers, *provided they are evenly distributed inside a nanocrystal*,

can deliver.

In brief, the numbers given above show that the task to realize single molecule FRET SNOM with NV color centers in nanodiamonds available for us is certainly demanding but could be realizable if one will work hard enough. During last five years, we regularly prepared FRET-active SNOM probes containing colored nanodiamond particles by dipping a sharp aperture SNOM fiber probe into a solution (acetone, chloroform, ethanol, DMSO) containing certain polymer (PMMA, chitosan, PDMS) at different concentrations and fluorescent ND with different sizes and NV centers concentrations, and extracting them (using different fashions to do so) from these solutions. After solvent evaporation, one has at hand an aperture SNOM probe which is covered by thin polymer layer with ND particles; the presence of the latter has been confirmed by fluorescent and kinetic measurements as well as by Scanning Electron Microscopy images. Examples of such FRET active probes are presented in Fig. 4. Earlier we prepared similar probes with dye molecules[12] and CdSe semiconductor nanocrystals[13] (we coined a name "self-sharpening pencil probe" for them), and this is exactly their exploitation which finally leads to obtaining of single molecule FRET SNOM images[17], while recording of such images at the level of tens and hundreds of molecules involved was almost routine.

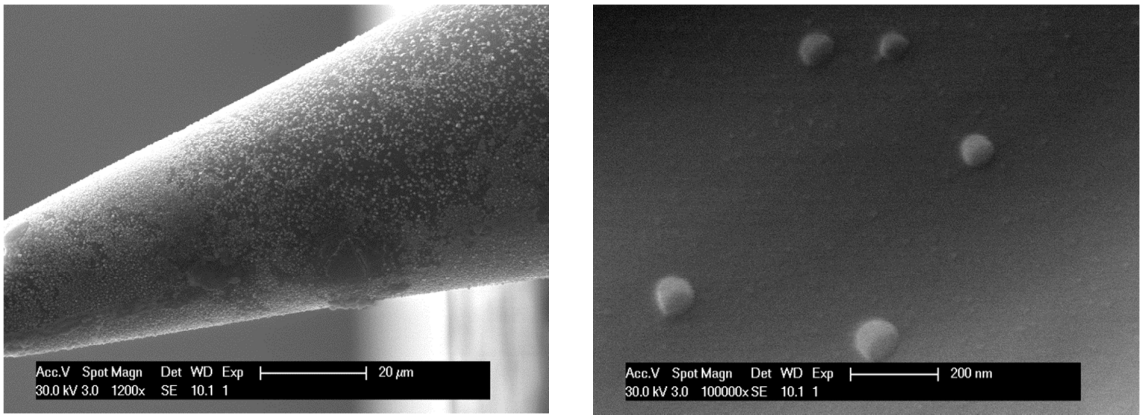

Fig. 4. Scanning Electron Microscopy images of SNOM probe surface covered with thin chitosan layer with fluorescent 40 nm-size nanodiamonds. In the right image, the obtaining of isolated individual ND particles with this approach is illustrated.

Nevertheless, despite all these efforts, we were unable to see FRET SNOM images with such probes and differently deposited layers of Oxazine 1, Oxazine 750 and Rhodamine 800 dyes[41] (calculated Förster radii range 4 – 6 nm) even at the aforementioned "many molecules" level. These experiments were performed exploiting excitation by nanosecond pulsed 532 nm laser and cw argon ion laser line at 514 nm; in all cases the necessary Kaiser Optical Systems (Ann Arbor, MI, USA) notch filter and appropriate set of long pass optical filters were exploited.

These probes were successfully used as local fluorescent probes, cf. Ref.[52]. What can be an explanation for this failure? Of course, due to the quite demanding character of the task, we cannot exclude that we simply did not work hard enough or were unlucky: it might happen that indeed no one probe prepared by us contains NV centers "correctly oriented" (close to that part of ND which touches the sample rather than an opposite part), or like. However, this does not seem too plausible for us, and as of today we are inclined to suggest the following explanation.

Recently, certain evidences appeared that nitrogen vacancies may be *unstable* if too close to the nanodiamond crystal surface. In particular, there is a theoretical prediction that NV centers are thermodynamically unstable in nanodiamonds less than 2 nm in size[53]. Further, strong blinking was detected for ND particles 5 nm in diameter[54], permanent bleaching of a material fraction of NV centers engineered 2-5 nm beneath the *F*-terminated diamond surface was reported[44], and so forth. In our opinion, this might be quite possible that for the distances of the order of 3 or so nanometers from the surface, NV centers might be unstable, or, more probable, have quite limiting time of life, possibly dependent on irradiation conditions (i.e. they might be subject to strong enough photobleaching). This suggestion would explain all our experimental observations; however, let us repeat again, at present we are not ready to claim that this is the only one possible explanation so that it is impossible to realize single FRET SNOM with NV centers in nanodiamonds.

To conclude this Section of the paper, we would like to make the following remarks. FRET observation between single approximately 20-nm size ND and infrared IRdye-800CW (the calculated Förster radius is equal to 5.6 nm) has been reported[55]. An analysis of this paper shows that here the fluorescent center is located somewhere close to the nanocrystal center, and large number of dye molecules, attached to the surface of this particle, are responsible for an observed FRET. Thus this is more a confirmation rather than rebuttal of our suggestion.

In this research, the authors used ND colored by 40 keV He^+ ion irradiation[56]. It is, of course, clear that much more bright particles can be obtained in such a way, and we not once attempted to produce such bright sources. For this, we started from liquid solution of 50 nm diamond particles in water with initial concentration of $7 \cdot 10^{12} - 7 \cdot 10^{10}$ particles/ml prepared by dissolving initial water (with some additives to prevent coagulation) solutions obtained from Microdiamant AG, Lengwill, Switzerland. 10 μl droplet of a solution was deposited onto a thin quartz plate, spread over the surface around 0.5 cm^2 and dried in air, afterwards these plates were immediately irradiated with He^+ ion beam, either of energy 1 MeV and dose $3 \cdot 10^{15}\ ion/cm^2$ in van der Graaf generator of Sevchenko Institute of Applied Physics Problems Belorussian State University, Minsk, Belarus; or of energy 130 keV, 500 keV or 1.7 MeV and typical dose 10^{15} ions/cm^2 in tandetrone accelerator of Indira Gandhi Center for Atomic Research, Kalpakkam, India. (Proton irradiation with energy of 1 MeV and similar doses also was attempted in India). After a few days these quartz plates were annealed in technical vacuum at 800^0 C during two hours. Based on data reported in Ref.[56] and other available data concerning defect

production in dielectrics by high energy ions, we estimated that in these conditions we should be close to the saturation, i.e. the most part of nitrogen vacancies could be transformed into fluorescent centers. These samples were indeed very bright, and single fluorescent nanodiamond crystals and/or clusters of ND particles "glued" together were easily seen in our SNOM when excited by 514 nm line of cw argon ion laser in transmission mode, see Fig. 5. Appropriate Kaiser Optical Systems (Ann Arbor, MI, USA) notch filter and a set of color filters cutting fluorescence shorter that 590 nm have been used during signal detection. Unfortunately, all attempts to "lift off" bright nanocrystal(s) from the quartz sample by "approach – (gentle) pressure – contraction" cycle[52,57] using bare or modified (for example, coated with thin poly-l-lysine layer) SNOM tip to prepare an active FRET SNOM tip grafted with ND crystal, failed. Attempts to observe FRET SNOM images with these samples using "self-sharpening pencil" aperture SNOM probes coated with thin layers of the aforementioned appropriate dyes[12] also were unsuccessful.

Second, besides NV centers in ND, other types of defects are now considered to be used in quantum informatics and could be prospective for FRET SNOM. Diamond contains more than 500 types of defect centers, and some of them look quite suitable, probably even more suitable than NV centres, for the task at hand. Analysis of the literature shows that, for example, chromium-related color centers, which possess narrow fluorescent line around 750 nm and for which the very large quantum efficiency was reported[58] look quite interesting. Similarly, Si-related color centers (narrow fluorescence line around 740 nm) look interesting as well. Recently, precisely the circumstance that the SiV centers, contrary to the NV centers, are stable and bright emitters in particles as small as 1.6 nm in size, became the main topic of research[59]; note also that these centers are theoretically predicted to be stable in such small crystals[60]. Similarly, Xe-related vacancies[61] can be considered, and so on. However, the questions of their thermodynamic stability when close to the nanoparticle surface, as well as detailed studies of photostability of all these color centers (which is usually claimed to be quite large but we failed to find exact data) and their quantum efficiency must be undertaken before further steps in this direction will become possible.

3.2. On the possibilities of FRET SNOM with rare earth ions in (nano)crystals

The efficiency of FRET or, better to say, the value of Förster radius, is independent on the donor dipole moment[3-5]. This is a prerequisite for the use of much more weak than dye molecules, semiconductor nanocrystals or colour centres, donors for single molecule FRET SNOM. If one is willing to use rare earth ions in crystals for this purpose (for many of optical transitions in them the quantum efficiency is close to 100% even at room temperatures[23-26]), due to the circumstance that their optical absorption/emission cross sections (dipole forbidden intraband *f-f* transitions) typically are roughly three orders of magnitude smaller than those pertinent for dyes[23-26], instead of thousands counts/s he or she will have a signal

only of the order of 10 counts/s (see eq. 1). Knowing that for relatively strong transitions of rare earth ions in crystals the fluorescence time ranges tens – two hundreds of microseconds, the exploitation of μs-duration laser pulses with the repetition rate around 100 Hz, i.e. something similar to what we actually used in our experiments with acousto-optical modulator[27], looks desirable and can lead to signal – noise ratio improvement overcoming the dark noise detector limit (see above; again, the total laser power at the SNOM fiber probe entrance should not exceed a few mW). But, of course, in any case such a low level of the signal presupposes slow scanning, and it is hard to say either such an approach is realizable and might be useful in practice.

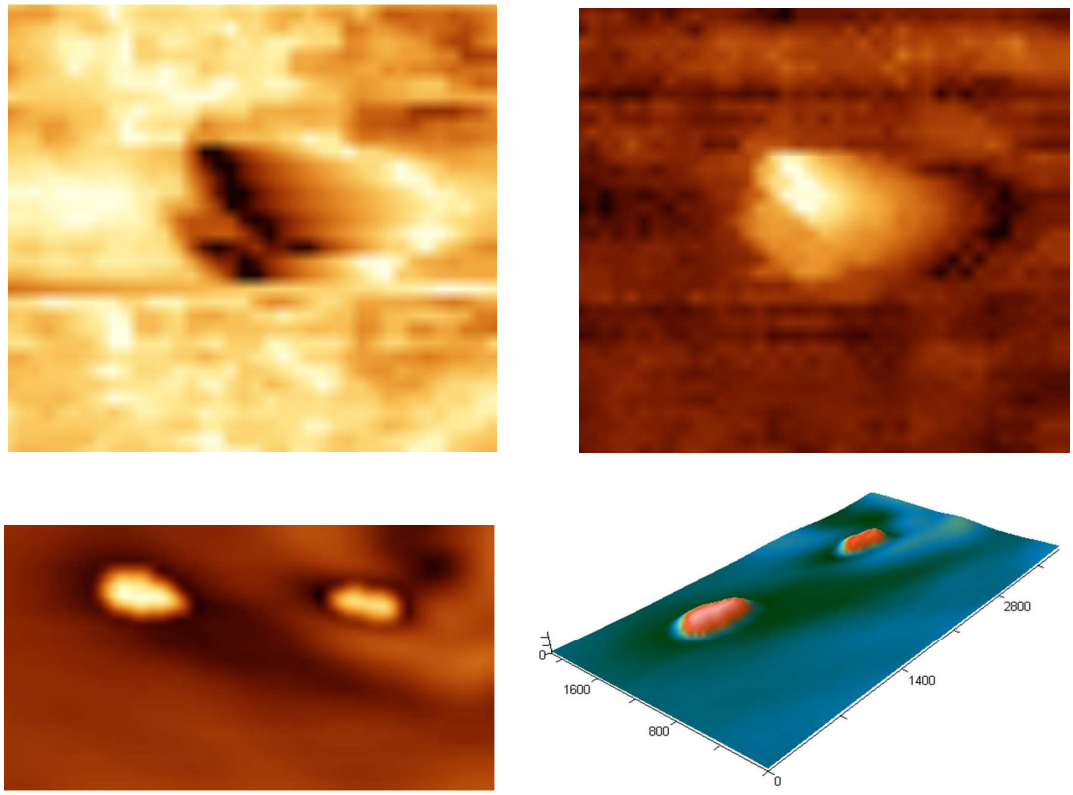

Fig. 5. Topographical (a) and near-field fluorescent (b) images of 50 nm-size diamond nanoparticles colored by 1.7 MeV He^+ ion irradiation in Kalpakkam, India; scan size: 150 x 150 nm. Near-field optical fluorescent image (c) and its 3D reconstruction (d) of the same particles colored by 130 keV He^+ ion irradiation in Kalpakkam, India; scan size 3.5 μm x 2 μm.

Certainly, optical *excitation* cross section of rare earth ion can be a few orders of magnitude larger than the corresponding optical absorption/emission cross section if the energy transfer from organic ligands or nanoparticle surrounding this ion is involved[23]. When can their use help? Due to the very nature of FRET, if a donor-acceptor distance is equal to the Förster distance R_0, the rate of energy transfer is

equal to that of the radiative decay hence the process of imaging at such distances remains slow. Interesting possibilities might appear if we are able to work at donor-acceptor distances, say, twice smaller than the R_0 value. This will lead to roughly 2^6 = 64 times increase of the FRET rate: consequently, one may observe a sufficiently strong FRET signal when the active ion of the SNOM probe is very close to an acceptor, and see nothing when there is no appropriate acceptor in its vicinity. Besides, the scanning rate also might be essentially increased, and all this certainly looks promising for FRET SNOM.

At present, we would not like to speculate more on this topic and will limit ourselves just with an indication of some optical transitions in rare earth ions in crystals which seem interesting for future work in this direction. The list might be not exhaustive and we did not search for optimal host matrices for the rare earth ions and optical transitions at question (being fully aware of the large importance of this question). Analysis of the literature enables to propose the following three transitions, each of which possesses optical emission cross section more than $10^{-19}\ cm^2$ and fluorescence time not exceeding 200 μs. First, this is the famous $^4F_{3/2}-^4I_{11/2}$ transition centred around 1.06 μm in Nd^{3+} ion; in some cases, transitions to the level neighbouring to $^4I_{11/2}$ might be used which gives rise to fluorescence wavelength around 880 nm. Then this is $^1D_2-^3H_4$ transition in Pr^{3+} ion centred around 600 – 606 nm, and, finally, $^3H_4-^3H_6$ transition in trivalent thulium ion centred around 795 nm. Famous and extremely important for telecommunication ca. 1.5 microns $^4F_{13/2}-^4F_{9/2}$ transition in erbium ion is strong but, besides being probably "too IR" for FRET SNOM purposes, also possesses quite long fluorescence times, $\geq 2\ ms$.

In this section we also would like to indicate one more interesting possibility. This is not *f-f* intraband transitions, but electric dipole allowed *f-d* transitions in some rare earth ions in crystals. Indeed, this is quite known that single (bivalent) samarium ion has been detected in CaF_2 crystal already in 1988[62] by observing *f-d* transition at 708 nm, but this was done at 77 K while at room temperature the quantum yield of the transition at question is prohibitively small. Situation is very different for three-valent Pr and Ce ions in different crystals, where even at room temperatures the quantum efficiency of *f-d* transition is close to unity[63] which, in particular, enabled recently to observe single praseodymium ion in YAG[64] and YSO[65] crystals. Different nanocrystals or nanoparticles containing these ions should be seriously considered as candidates for single molecule FRET SNOM in UV and violet-blue spectral regions. Indeed, the reported parameters of e.g. $LiCaAlF_6:Ce^{3+}$ lasing medium, viz. optical emission cross section $\sigma = 6.8 \cdot 10^{-18}\ cm^2$ and fluorescence time 50 ns (band 280 – 315 nm)[58], show that the corresponding systems should be quite comparable with FRET SNOM probes exploiting dye molecules (but we hope much more photostable). Of course, a lot of things still should be clarified (including an influence of nanoparticle surface on FRET and details of UV SNOM

construction), but actually the research aiming the use of $LaF_3:Pr^{3+}$ and $LaF_3:Ce^{3+}$ nanoparticles (lasing in $LaF_3:Ce^{3+}$ crystals also has been reported[66]) made by microwave-hydrothermal technique[67] as FRET SNOM probes has already started.

4. Single Molecule coherent FRET SNOM at liquid helium temperature

In the Introduction, we have already mentioned that for many rare-earth ions in crystals at liquid helium temperature, inter-ion FRET is a *coherent* process and electronic excitation energy flows back and forth between donor and acceptor, having dipole moments d_D and d_A respectively and located at a distance r from each other, with the characteristic time[22]

$$T_{FRET} = \frac{\pi\hbar r^3}{\alpha\kappa d_D d_A} \qquad (2).$$

Here α and κ are respectively geometrical and spectral factors (of the order of 1) which take into account the mutual orientation of two dipoles and their spectral overlapping. Accepting d_D=d_A we obtain the following estimation of the coherent FRET Förster radius where the FRET rate is equal to that of radiative decay:

$$r = \left(\frac{3\alpha\kappa\eta}{8\pi^5}\right)^{1/3} \lambda \qquad (3).$$

Here λ is the wavelength and η takes into account the ratio between the radiation decay time T_1 and transverse relaxation time T_2, $T_2 = \eta T_1$. We argued that in typical cases this radius is around 20 nm[22] (afterwards this simple calculation has been confirmed by rigorous quantum electrodynamics treatment[68]) so that, given also the characteristic microsecond-range decoherence times, the process can be controlled by modern Scanning Probe Microscope working at liquid helium temperature. Using a pseudospin ½ model (excited state of an ion corresponds to the state with the pseudospin *z*-projection equal to +1/2, unexcited to -1/2) and its generalizations for systems involving many interacting dipoles[69,70], protocols how to create qubits in well-defined quantum states and how to realize CC…CNOT operators were proposed[22]. Later on, we reported first experiments in the field (photon echo researches in M-pair centers of Nd^{3+} ions in calcium fluoride; interion interaction in this system is exactly the coherent dipole-dipole interaction we are interested in)[69] and proposed their continuation[70]. Quite recently, the possibility of *coherent cooperative* FRET process in rare earth ions has been predicted[71].

Certainly, experiments in this field require sophisticated SNOM arrangement. The appropriate device should not only simply work at liquid helium temperature, but it should be capable to fast and precise scanning necessary e.g. for addressing certain pre-selected (groups of) rare-ion ions or like, cf. Refs.[22,69,70]. Analysis of the literature shows that this problem, albeit difficult indeed, still can be solved and a few earlier discussed low temperature SNOM devices[72-74] look suitable for the task. In our case, we plan to use the recently constructed and available for joint work

SNOM[75,76] which construction is rather similar to our SNOM[27,28]. It also exploits proprietary double-resonance optical fiber probe montage onto quartz tuning fork (thus proven to work at low helium temperature) so that this microscope has the same advantages including the fast scanning which makes it especially suitable for the realization of the aforementioned quantum informatics-related experiments.

As a first application, we are considering an experiment demonstrating the possibility of entanglement of two spatially separated macroscopic bodies, viz. small microcrystals containing rare-earth ions. SNOM tip and sample which are presented in the Figure 1, left, can be used for illustration, but now we suppose that the sample is, say, $LiYF_4$:Er single crystal with the concentration of Er ions ca. 0.1 at% while other similar $LiYF_4$:Er single crystal having a few microns size is attached onto a SNOM tip; all setup has a liquid helium temperature. (This particular crystal is selected because it is characterized by especially small ratio of inhomogeneous to homogeneous spectral line broadening[77]). With suitable laser excitation, numerous pairs of ions (donors and acceptors) divided between these two microcrystals are subject to coherent dipole-dipole interactions (FRET). It can be shown that starting from two microcrystals at contact and disengaging after the end of laser pulse irradiation (by applying an appropriate HV electric pulse onto a *z*-piezo carrying SNOM probe), one is able to entangle up to millions of rare-earth ions belonging to two different macrobodies (microcrystals).

For above estimation, we supposed an application of time-varying electric potential onto the SNOM tip to make, exploiting Stark shift of erbium ion optical transition frequency[78], different donor – acceptor pairs resonant with each other. It is worthwhile to note that the possibility to exploit local Stark-induced resonance dipole-dipole interactions for coherent optical dipole coupling of two perrylene molecules has been demonstrated earlier[79].

At the current state of researches, it would be premature to discuss in details also other planned combinations of FRET SNOM with such Quantum Information Processing approaches as the nanolocally-controlled frequency schifts[80,24] and Coherent Reversible Inhomogeneous Broadening of dopant ion spectral line[81,24]. Still we believe that this very short account well demonstrates interesting and exciting perspectives of coherent FRET SNOM approach for quantum computing and related topics.

Conclusion

First, we have discussed the current state of single molecule FRET SNOM for room temperature case. Despite the circumstance that our hopes to profit from ultrahigh photostability of NV color centers in nanodiamond crystals still did not result in the preparation of FRET-active SNOM probes containg single fluorescent center at the apex suitable for everyday use, there are many indications that this task can be solved with (may be other than NV) color centers in nanodiamonds and rare-earth ions in crystals. Importance of the practical realization of the proposed

method, in our opinion, is evident and needs not to be discussed at length.

We have also discussed novel possibilities concerning quantum informatics applications of coherent FRET SNOM at liquid helium temperature. Here we profit a lot from the circumstance that, in comparison with 2003 when our proposal has been put forward[22], the number of papers discussing possible quantum computing applications of rare earth ions in crystals virtually exploded, and it became much easier to search for appropriate crystals and optical transitions to be used. In particular, this enabled to elaborate sufficiently detailed scheme of an experiment aiming the demonstration of entanglement of two macroscopic bodies, very briefly presented in the paper, as well as some other ideas.

The authors would like to thank M. Petrova and K. Keevend for help with FRET SNOM experiments, and I. Sildos for useful discussions of color centers in ND properties. We are grateful to Swiss National Science Foundation for financial support of these researches during a number of years including the latest grant N 200020-149424.

References

1. S. K. Sekatskii and V. S. Letokhov, *Appl. Phys*. B**63**, 1996, 525.
2. S. K. Sekatskii, Fluorescence Resonance Energy Transfer Scanning Near-Field Optical Microscopy, In *Nano-Optics and Near-Field optical Microscopy*, ed. A. Zayats and D. Richards, Artech, London, 2009.
3. V. M. Agranovich and M. D. Galanin, *Electron excitation energy transfer in condensed matter*, Amsterdam, North Holland, 1982.
4. R. M. Clegg, Fluorescence resonance energy transfer, In *Fluorescence imaging spectroscopy and microscopy*, ed. X. F. Wang and B. Herman, New York, John Wiley and sons, 1996.
5. E. A. Jares-Erijman and T. M. Jovin, *Nature Biotech.*, 2003, **21**, 1387.
6. M. Ohtsu, *Near-field nano/atom optics and technology*, Tokyo, Springer, 1998.
7. R. C. Dunn, *Chem. Rev*., 1999, **99**, 2891.
8. L. Novotny and B. Hecht, *Principles of nano-optics*, Cambridge, Cambridge Univ. Press, 2006.
9. S. A. Vickery and R. C. Dunn, *Biophys. J*., 1999, **76**, 1812.
10. G. T. Shubeita, S. K. Sekatskii, M. Chergui, G. Dietler and V. S. Letokhov, *Appl. Phys. Lett*., 1999, **74**, 3453.
11. S. A. Vickery and R. C. Dunn, *J. Microsc.*, 2001, **202**, 408.
12. G. T. Shubeita, S. K. Sekatskii, G. Dietler and V. S. Letokhov, *Appl. Phys. Lett.*, 2002, **80**, 2625.
13. G. T. Shubeita, S. K. Sekatskii, G. Dietler, I. Potapova, A. Mews and T. Basché, *J. Microsc*., 2003, **210**, 274.
14. Y. Ebenstein, T. Mokari and U. Banin, *J. Phys. Chem. B,* 2004, **108**, 93.
15. F. Müller, S. Götzinger, N. Gaponik, H. Weller, J. Mlynek and O. Benson, *J.*

Phys. Chem. B, 2004, **108**, 14527.
16. S. K. Sekatskii, G. Dietler, F. Bonfigli, S. Loreti, T. Marolo and R. M. Montereali, *J. Lumines*., 2007, **122-123**, 362.
17. S. K. Sekatskii, G. Dietler and V. S. Letokhov, *Chem. Phys. Lett.*, 2008, **452**, 220.
18. R. Schirhagl, K. Chang, M. Loretz and C. L. Degen, *Ann. Rev. Phys. Chem*., 2014, **65**, 83.
19. I. Aharonovich, S. Castelletto, D. A. Simpson, C.-H. Su, A.-D. Greentree and S. Prawer, *Rep. Prog. Phys*., 2011, **74**, 076501.
20. F. Jelezko and J. Wrachtrup, *Phys. Stat. Solidi*, 2006, A**203**, 3207.
21. S. Pezzagna, D. Rogalla, D. Wildanger, J. Meijer and A. Zaitsev, *New J. Phys*., 2011, **13**, 035024.
22. S. K. Sekatskii, M. Chergui and G. Dietler, *Europhys. Lett*., 2003, **63**, 21.
23. G. Liu and B. Jacquier, *Spectroscopic properties of rare earths in optical materials*, Springer, Berlin, 2005.
24. P. Goldner, A. Ferrier and O. Guillot-Noel, *Handbook on the Physics and Chemistry of Rare Earth,* 2015, **46**, 1.
25. C. W. Thiel, T. Böttger and R. L. Cole, *J. Lumines*., 2011, **131**, 353.
26. T. T. Basiev, I. T. Basieva, A. A. Kornienko, V. V. Osiko, K. K. Pukhov and S. K. Sekatskii, *J. Mod. Opt*., 2012, **59**, 166.
27. D. V. Serebraykov, S. K. Sekatskii, A. P. Cherkun, K. Dukenbayev, I. V. Morozov, V. S. Letokhov and G. Dietler, *J. Microsc*., Pt. 2, 2008, **229**, 287.
28. A. P. Cherkun, D. V. Serebryakov, S. K. Sekatskii, I. V. Morozov and V. S. Letokhov, *Rev. Sci. Instr*., 2006, **77**, 033703.
29. D. V. Serebryakov, A. P. Cherkun, B. A. Loginov and V. S. Letokhov, *Rev. Sci. Instr*., 2002, **73**, 1795.
30. H. Chibani, K. Dukenbayev, M. Mensi, S. K. Sekatskii, and G. Dietler, *Ultramicroscopy*, 2010, **110**, 211.
31. M. Mensi, G. Mikhailov, S. Pyatkin, J. Adamcik, S. Sekatskii, and G. Dietler, SPIE Proceedings, 2010, **7712**, 771222.
32. R. Stöckle, C. Fokas, V. Deckert, R. Zenobi, B. Sick, B. Hecht and U. P. Wild, *Appl. Phys. Lett*., 1999, **75**, 160.
33. A. Sayah, C. Philipona, P. Lambelet, M. Pfeffer and F. Marquis-Weible, *Ultramicroscopy*, 1997, **71**, 59.
34. J. Adamcik, F. Valle, G. Witz, K. Rechendorff and G. Dietler, *Nanotechnology*, 2008, **19**, 38.
35. S. Kühn, S. Hettich, S. Schmitt, J.-Ph. Poizat and V. Sandoghdar, *J. Microsc*., 2000, **202** Pt.1, 2.
36. E. Rittweger, K. Y. Han, S. E. I. Irvine, C. Eggeling and S. W. Hell, *Nat. Photonics*, 2009, **3**, 144.

37. S. Arroyo-Camejo, M.-P- Adam, M- Besbes, J.-P- Hugonin, V. Jacques, J.–J. Greffet, J.-F. Roch, S- W. Hell and F. Treussart, *ACS Nano*, 2013, **7**, 10912.
38. A. Gali, *Phys. Rev*., 2009, B**79**, 235210.
39. T. Gaebel , M. Domhan, C. Wittmann, I. Popa, F. Jelezko, J. Rabeau, A. Greentree, S. Prawer, E. Trajkov, P. R. Hemmer and J. Wrachtrup, *Appl. Phys. B: Lasers Opt*., 2006, **82**, 243.
40. K. Iakubovskii, G. J. Adriaenssens and M. Nesladek, *J. Phys.: Condens. Mattter*, 2000, **12**, 189.
41. U. Brackmann, *Lambdachrome laser dyes*, Lambda Physik GmbH, Goettingen, 1997.
42. C. Santori, P. E. Barclay, K.-M. C. Fu and R. G. Beausoleil, *Phys. Rev. B*, 2009, **79**, 125313.
43. L. Rondlin, G. Dantelle, A. Slablab, F. Grosshans, F. Treussart, P. Bergonzo, S. Perruchas, T. Gacoin, M. Chaigneau, H.-C. Chang, V. Jacques and J.-F. Roch, *Phys. Rev.*, 2010, B **82**, 115449.
44. K. Ohashi, T. Rosskopf, H. Watanabe, M. Loretz, Y. Tao, R. Hauert, S. Tomizawa, T. Ishikawa, J. Ishi-Hayase, S. Shikata, C. L. Degen and K. M. Itoh, *Nano Lett.*, 2013, **13**, 4733.
45. M. Kaviani, P. Deak, B. Aradi, T. Frauenheim, J.-P. Chou and A. Gali, Nano Lett., 2014, **14**, 4772.
46. I. I. Vlasov, O. Shenderova, S. Turner, O. I. Lebedev, A. A. Basov, I. Sildos, M. Rähn, A. A. Shiryaev and G. Van Tendeloo, *Small*, 2010, **6**, 687.
47. G. Dantelle, A. Slablab, L. Rondin, F. Lainé, F. Carrel, Ph. Bergonzo, S. Perruchas, T. Gacoin, F. Treussart and J. E. Roch, *J. Luminesc*., 2010, **130**, 1655.
48. G. Davies and M. F. Hamer, *Proc. R. Soc. Lond*., 1976, A**348**, 285.
49. A. Bevaratos, R. Brouri, T. Gacoin, J.-P. Poizat and P. Grangier, 2001, *Phys. Rev.* A**64**, 061802R.
50. A. Gruber, A. Dräbenstedt, C. Tietz, L. Fleury, J. Wrachtrup and C. Von Borczyskowki, 1997, *Science*, **276**, 2012.
51. T. L. Wee, Y. K. Tzeng, C. C. Han, H. C. Chang, W. Fann, J. H. Hsu, K. M. Chen and Y. C. Yu, *J. Phys. Chem*., 2007, A**111**, 9379.
52. A. Drezet, Y. Sonnefraud, A. Cuche, O. Mollet, M. Berthel and S. Huant, *Micron*, 2015, **70**, 55.
53. A. S. Barnard and M. Sternberg, *J. Phys. Chem*., 2005, B**109**, 17107.
54. C. Bradac, T. Gaebel, N. Naidoo, M. J. Sellars, J. Twamley, L. J. Brown, A. S. Barnard, T. Plakhotnik, A. V. Zvyagin and J. R. Rabeau, *Nature Nanotech*., 2010, **5**, 345.
55. Y.-Y. Chen, H. Shu, Y. Kuo, Y.-K. Tzeng and H.-H. Chang, *Diamond Rel. Mat*., 2011, **20**, 803.
56. Y.-R. Chang, H.-Y. Lee, K. Chen, C.-C. Chang, D.-S. Tsai, C.-C. Fu, T.-S. Lim, Y.-K. Tzeng, C.-C. Fang, C.-C. Han, H.-H. Chang and W. Fan, *Nature Nanotech*. 2008, **3**, 284.

57. A. Cuche, A. Drezet, Y. Sonnefraud, O. Faklaris, F. Treussart, J. F. Roch and S. Huant, *Opt. Express*, 2009, **17**, 19969.
58. I. Aharonovich, S. Castelletto, D. A. Simpson, A. Stacey, J. McGallum, A. D. Greentree and S. Prawer, *Nano Lett*., 2009, **9**, 3195.
59. I. I. Vlasov, A. A.Shiryaev, T. Rendler, S. Steinert, S.-Y. Lee, D. Antonov, M. Vörös, F. Jelezko, A. V. Fisenko, L. F. Semjonova, J. Biskupek, U. Kaiser, O.I. Lebedev, I. Sildos, P. R. Hemmer, V. I. Konov, A. Gali and J. Wrachtrup, *Nature Nanotech*., 2014, **9**, 54.
60. A. S. Barnard, I. I. Vlasov and V. G. Ralchenko, *J. Mater. Chem*., 2009, **19**, 360.
61. Y. Deshko and A. Gorokhovsky, *Phys. Stat. Solidi. B*, 2013, 250, 278.
62. R. Lange, W. Grill and W. Martienssen, *Europhys. Lett*., 1988, **6**, 499.
63. M. J. Weber, *Solid State Comm*. 1973, **12**, 741.
64. R. Kolesov, K. Xia, R. Reuter, R. Stöhr, A. Zappe, P. R. Hemmer and J. Wrachtrup, *Nature Comm*., 2012, **3**, 1029.
65. T. Utikal, E. Eichhammer, L. Petersen, A. Renn, S. Götzinger and V. Sandoghdar, *Nature Comm*., 2014, **5**, 3627.
66. D. J. Ehrlich, P. F. Moulton and R. M. Jr. Osgood, *Opt. Lett*., 1979, **4**, 184.
67. A. S. Vanetsev, E. V. Samsonova, O. M. Gaitko, K. Keevend, A. V. Popov, U. Mäeorg, H. Mändar, I. Sildos and Yu. V. Orlovskii, *J. Alloy. Compound*., 2015, **639**, 415.
68. V. V. Klimov, S. K. Sekatskii and G. Dietler, *J. Mod. Opt*., 2004, **51**, 1919.
69. S. K. Sekatskii, T. T. Basiev, I. T. Basieva, G. Dietler, V. V. Fedorov, A. Ya. Karasik, Yu. V. Orlovskii and K. K. Pukhov, *Opt. Comm*., 2006, **259**, 298.
70. I. T. Basieva, T. T. Basiev, G. Dietler, K. K. Pukhov and S. K. Sekatskii**,** *Phys. Rev.* B., 2006, **74**, 165329.
71. S. K. Sekatskii and K. K. Pukhov, *Opt. Spectrosc*., 2014, **117**, 902.
72. J. Michaelis, C. Hettich, J. Mlynek and V. Sandoghdar, *Nature*, 2000, **405**, 325.
73. M. Gregor, R. Henze, T. Schroder and O. Benson, Appl. Phys. Lett., 2009, **95**, 153110.
74. M. Skacel, M. Francardi, A. Gerardino, B. Alloing, L. Li and A. Fiore, *J. Phys: Conf. Ser.*, 2010, **245**, 012040.
75. M. G. Petrova, G. V. Mishakov, E. I. Demikhov and A. I. Sharkov, *Bull. Lebedev Phys. Inst*., 2010, **37**, 276.
76. V. V. Prokhorov, M. G. Petrova, S. I. Pozin, N. N. Kovaleva and E. I. Demikhov, C*urrent Nanoscience*, 2014, **10**, 700.
77. R. M. Macfarlane, A. Cassanho, R. S. Meltzer, *Phys. Rev. Lett.* **69** (1992) 542.
78. R. M. Macfarlane, *J. Luminesc*, **125**, 156 (2007).
79. C. Hettich, C. Scmitt, J. Zitzmann, S. Kühn, I. Gerhardt and V. Sandoghdar, *Science*, 2002, **298**, 385.
80. N. Ohlsson, R. Monah, and S. Kroell, *Opt. Com*., 2002, **201**, 71.
81. A. L. Alexander, J. J. Longdell, M. J. Sellars and N. B. Manson, *Phys. Rev. Lett*., 2006, **96**, 043602.